

EXPERIMENTAL AND SIMULATION STUDY OF A PERMANENT MAGNET D.C MOTOR AT STEADY STATE

Salah. I. S. TNATIN(1), Seliman A. MOHAMED (2) and Fatma. R. M. ABDALATI (3)

(1) Assistant lecturer at, Department of Electrical Engineering, Omar Al-Mukhtar University, Albayda, Libya

salah.tnatin@omu.edu.ly

(2) Assistant lecturer at Department of Electrical Engineering, Omar Al-Mukhtar University, Albayda, Libya

seliman.mohamed@omu.edu.ly

(3) Assistant lecturer at Department of Electrical Enginemen, Higher Institute for Comprehensive Careers, Albayda, Libya fatmaabdalati@gmail.com

ABSTRACT

This paper studies and investigates of the performance of permanent magnet D.C motors (PMDC motors) as well as determining the parameters of this type of motors at steady state. The study was carried out in two stages. The first stage involved the practical experimental to determine the parameters and characteristics of PMDC motor at steady state while the second stage centered on the simulation of mathematical modeling of this system using Simulink environment in MATLAB.. The best significant results show that the computer simulations provide results closely to values of experimental measurements, therefore it can be used to investigate the performance of PMDC motors and their characteristics. In addition, the efficiency of PMDC motor is higher than Electromagnetic D.C motors, also the damping coefficient has a negative effect on characteristics of motor especially at no-load steady state in spit of smallness value.

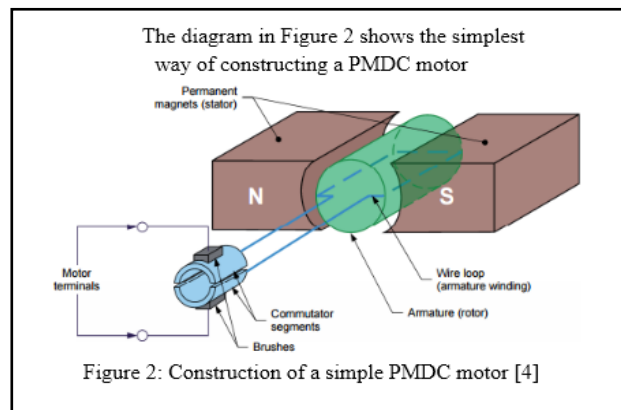
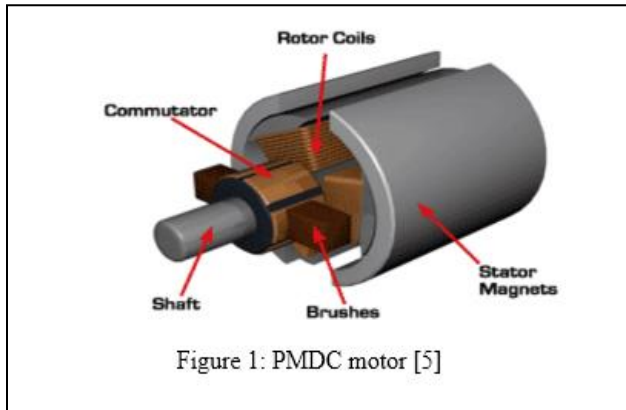
1. INTRODUCTION

The DC motor is one of the first machines used to convert electrical power into mechanical Power [1-2]. The DC motor uses electricity and a magnetic field to produce torque, which gives rotational speed. There are different kinds of D.C. motors, but they all work on the same principles [1-9]. Basic working principle of DC motor is based on the fact that whenever a current carrying conductor is placed inside a magnetic field, there will be mechanical force experienced by that conductor. Hence for constructing a DC motor it is essential to establish a magnetic field. The magnetic field is obviously established by means of a magnet. The magnet can be an electromagnet or permanent magnet. When a permanent magnet is used to create a

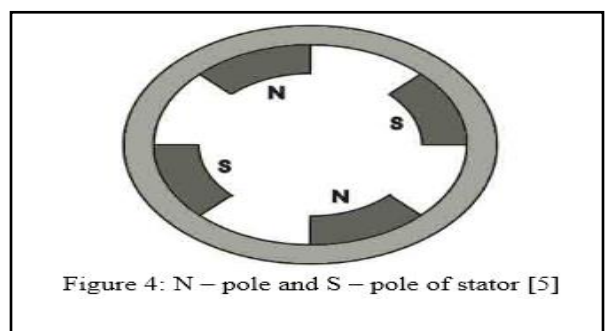
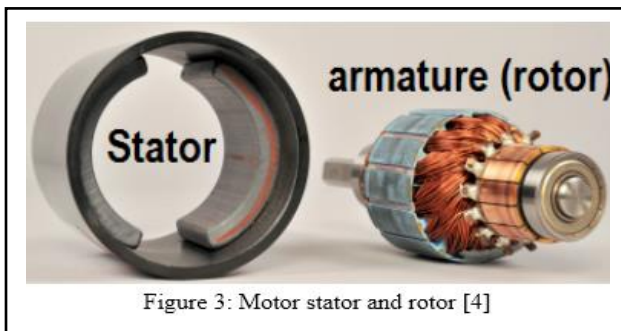
magnetic field in a DC motor, the motor is known as permanent magnet dc motor or PMDC motor. The PMDC Motors do not require field windings, they do not have field circuit copper losses thus they used where there is no need for speed control of the motor by means of controlling its field. This increases their efficiency [2-5]. In addition, they have a small size and cheaper. On the other hand, Permanent magnets cannot produce a high flux density as that as an externally supplied shunt field does. Also, the magnetic field of PMDC motor is present at all time, even when the motor is not being used. The PMDC motors are used in different applications ranging from fractions to several horse powers. They are developed up to about 200 kW for use in many industries. PMDC motors are mainly used in automobiles to operate windshield wipers and washers, to raise the lower windows, to drive blowers for heaters and air conditioners. They are also used in computer drives, toy industries, electric toothbrushes, portable vacuum cleaners, food mixers, wheelchairs, door openers and other applications [5]. The rest of the paper is organized as follows: Section 2 presents construction of PMDC motor. Section 3 presents mathematical model of PMDC motor that gives equivalent behavior for motor performance. Section 6 and 7 presents the experimental and simulation results of motor characteristics at steady state and in Section 8, the conclusion is discussed.

2. CONSTRUCTION OF PMDC MOTOR

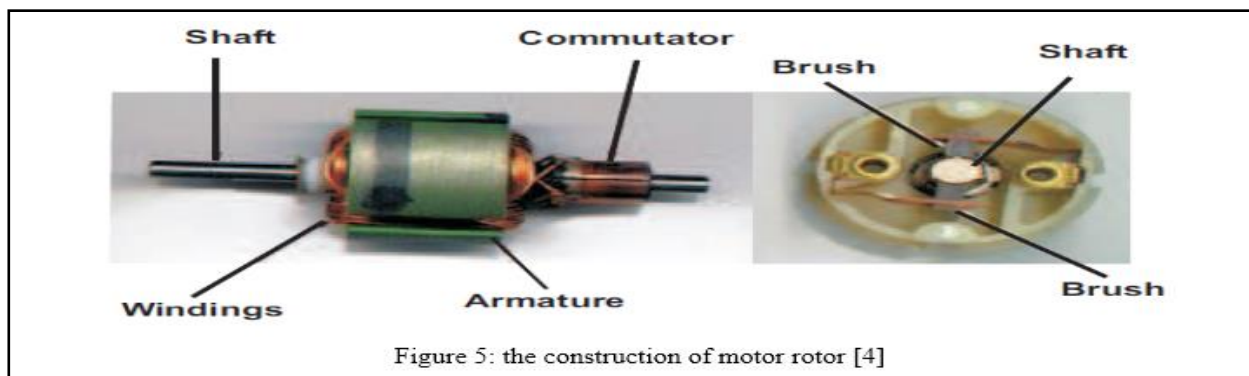
This type of motor is shown in Figure 1



PMDC motor mainly consists of two parts. A stator and an armature (rotor) as shown in Figure 3. The stator is usually made from steel in cylindrical form. The permanent magnets (located in stator) provide a magnetic field, instead of the stator winding. The permanent magnets are mounted in such a way that the N – pole and S – pole of each magnet are alternatively faced towards armature as shown in Figure 4.



The rotor or armature of PMDC motor also consists of a core, windings, and commutator. The rotor is made from layers of laminated silicon steel to reduce eddy current losses. Ends of armature winding are connected to commutator segments on which the brushes rest. The commutator is made from copper and brushes are usually made from carbon or graphite. DC supply is applied across these brushes. The commutator is in segmented form to achieve unidirectional torque. The reversal of direction can be easily achieved by reversing the polarity of the applied voltage. Figure 5 shows the construction of motor rotor.



3. MATHEMATICAL MODEL OF PMDC MOTOR

In order to study the steady state of PMDC motor, there are many applications for modeling the state that gives a description of system characteristics. The motor will reach full speed at steady state if the DC power supply is connected to motor terminal and the dynamic effects fall off and become zero.

3.1 ELECTRICAL CHARACTERISTICS OF PMDC MOTOR

PMDC motor is similar to other DC motor. Figure 6 shows the equivalent circuit for an ideal PMDC motor at no load steady state. V_a represents the applied voltage which causes the armature current I_a to flow, R_a is the resistance of the armature, and V_b is the generated or induced the back electromotive force, EMF voltage in the armature [6-8]. Motors convert electrical energy into mechanical energy. In ideal motor the basic relationship between electrical energy and mechanical energy is equal.

Mechanical energy = electrical energy

$$T_m * \omega_m = V_b * I_a \dots \dots \dots (1)$$

Where: T_m is the torque on the rotating shaft, ω_m is the rotational velocity of the armature. In real motor, input power is always higher than the output power, and rotational velocity is directly proportional to the back EMF V_b

$$V_b = K_b * \omega_m \dots \dots \dots (2)$$

Where: K_b is the back EMF constant of the motor. Figure 7 shows the equivalent circuit for PMDC motor with mechanical load.

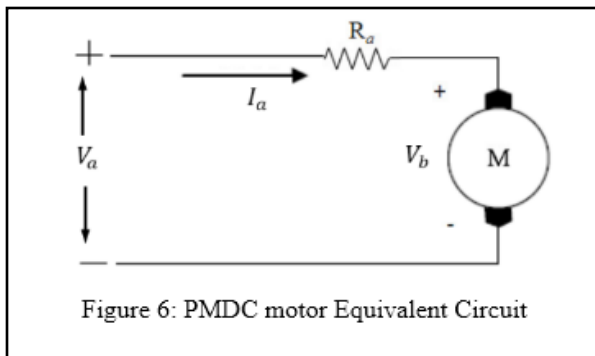


Figure 6: PMDC motor Equivalent Circuit

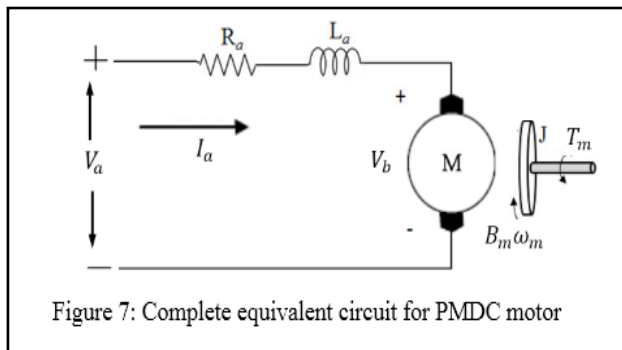


Figure 7: Complete equivalent circuit for PMDC motor

Applying Kirchhoff's law around the electrical loop by summing voltages throughout the circuit gives:

$$V_a - V_{Ra} - V_{La} - V_b = 0 \dots \dots \dots (3)$$

$$V_{Ra} = I_a R_a \quad , \quad V_{La} = L_a \frac{di_a}{dt}$$

Where: V_{Ra} is the voltage drop across the armature resistance, and V_{La} is the voltage drop across the inductance. Substituting in equation (3) and rearranging to obtain the differential equation that describes the electrical characteristics of PMDC motor

$$V_a - I_a R_a - L_a \frac{di_a}{dt} - K_b \omega_m = 0 \dots \dots \dots (4)$$

The $L \frac{di_a}{dt}$ term is ignored at the steady state, hence equation (4) can be rewritten as the following

$$V_a - I_a R_a - K_b \omega_m = 0 \dots \dots \dots (5)$$

The armature current can be calculated from equation (5) as following

$$I_a = \frac{V_a - K_b \omega_m}{R_a} \dots \dots \dots (6)$$

3.2 MECHANICAL CHARACTERISTICS OF PMDC MOTOR

For the mechanical characteristics of PMDC motor, performing an energy balance on the system, the sum of the torques of the motor must equal zero.

$$T_m - T_J - T_{Bm} - T_L = 0 \dots \dots \dots (7)$$

Where T_m is the electromagnetic torque, T_J is the torque due to rotational acceleration of the rotor, T_{Bm} is the torque produced from the velocity of the rotor, and T_L is the torque of the mechanical load. The electromagnetic torque, T_m is directly proportional to the armature current and can be written as

$$T_m = K_t * i_a \dots \dots \dots (8)$$

Where K_t is the torque constant, and dependent on the flux density of the fixed magnets, the reluctance of the iron core, and a number of turns in the armature winding. In metric (SI) units $K_t \left(\frac{N.M}{A} \right)$ is equal to $K_b \left(\frac{Volts}{rad/sec} \right)$ as justified in the literature [*]. T_J can be written as

$$T_J = J \frac{d\omega_m}{dt} \dots \dots \dots (9)$$

Where J is the inertia of the rotor. T_{Bm} is written as

$$T_{Bm} = B_m * \omega_m \dots \dots \dots (10)$$

Where B_m is the damping coefficient. Substituting equations (7),(8),and (9) into equation (10) gives the following differential equation

$$Kt * i_a - J \frac{d\omega_m}{dt} - B_m * \omega_m - T_L = 0$$

$$T_L = Kt * i_a - J \frac{d\omega_m}{dt} - B_m * \omega_m \dots \dots (11)$$

We not that the increased armature current will lead to an increase of the electromagnetic torque on the rotating shaft and it becomes higher than T_L , T_J , and T_{Bm} . After ignoring T_J at steady state the equation (11) can be written as

$$T_L = Kt * i_a - B_m * \omega_m \dots \dots \dots (12)$$

In case, no load attached the electrical losses can be represented by armature current and mechanical losses represented by damping coefficient at, also the torque of the mechanical load is zero, hence equation (12) can be rewritten as the following

$$Kt * i_a - B_m * \omega_m = 0 \dots \dots \dots (13)$$

The damping coefficient can be computed from equation (13) as

$$B_m = \frac{Kt * i_a}{\omega_m} = \frac{T_m}{\omega_m} \dots \dots \dots (14)$$

To obtain the relationship between T_L and ω_m , it can substitute I_a in equation (6) in equation (12) and rearranging the term

$$T_L = Kt * \left(\frac{V_a - K_b \omega_m}{R_a} \right) - B_m \omega_m$$

$$T_L = \frac{K_t * V_a}{R_a} - \omega_m \left(\frac{K_t K_b}{R_a} + B_m \right) \dots \dots \dots (15)$$

$M = \frac{K_t}{R_a} = \text{constant}$, $N = \frac{K_t K_b}{R_a} + B_m = \text{constant}$. Equation (15) shows the relationship between T_L and ω_m is a straight line, if the terminal voltage V_a and N are kept constant [10]

4. POWER IN PMDC MOTOR

The power input to a PMDC motor is basically the input current I_a multiplied by the applied voltage

$$\text{Input power } (P_{in}) = V_a * I_a \dots \dots (16)$$

Due to electrical and mechanical losses in the motor, the mechanical power out of the motor must be less than the electrical power in [7-10]. The most observable electrical loss is due to the armature resistance, $P_{elecloss} = I_a^2 R_a$. Power losses also occur due to friction between parts of the machine, magnetic inefficiencies of the material used air resistance of the rotating armature small resistance across the brushes used to couple current into the commutator. These losses can be

estimated together by specifying a total value for mechanical power lost, $P_{mechloss}$. The electrical power input to a PMDC motor must equal the sum of the mechanical power output and the different loss mechanisms.

$$P_{in} = P_{out} + P_{elecloss} + P_{mechloss} \dots \dots \dots (17)$$

The output power can be computed from the power balance equation (17), or from the product of output torque (T_L) and rotational velocity (ω_m) as

$$P_{out} = T_L * \omega_m \dots \dots \dots (18)$$

The output power is zero at no-load current (I_{a0}) and short-circuits current (I_{asc}) [10]

5. EFFICIENCY OF PMDC MOTOR

Efficiency, η of a system can be generally defined as the ratio of power output relative to power input. In DC motors this becomes the mechanical power out relative to the electrical power in:

$$\eta = \left(\frac{P_{out}}{P_{in}} \right) * 100\% \dots \dots \dots (19)$$

6. EXPERIMENTAL MEASUREMENTS

This part deals with measurement procedures which aim to achieve the requirements of the current search through the practical side. At steady state parameters of the PMDC motor R_a, K_b, K_t , and B_m are measured and computed while characteristics curves of the PMDC motor are plotted. The PMDC was unloaded and fed to 24 volts and the rotational velocity was measured using non – contacting tachometer. The armature current and the back EMF were measured under this no load condition. The measured readings were taken and recorded at different inputs as shown in Table 1.

Table 1: Experimental measurement data at steady state no load condition

No Load. V_{in} (V)	24	23	22	20	19	18	17
No Load. V_b (V)	22.72	21.1	20.23	18.4	17.47	16.75	16
No Load. I_a (A)	0.5	0.49	0.45	0.4	0.39	0.37	0.3
No Load. N (rpm)	1400	1300	1200	1100	900	700	600
$\omega_m \left(\frac{rad}{sec} \right) = N(rpm) * \left(\frac{2\pi}{60} \right)$	146.6	136	125.6	115.2	94.24	73.30	62.83

From Table 1 it can compute K_b and K_t for any reading, there were calculated as

$$K_b = \frac{V_b}{\omega_m} = \frac{22.72}{146.6} = 0.155 \left(\frac{Volt}{rad/sec} \right). \quad \text{Hence, } K_b = K_t = 0.155 \frac{N.M}{A}$$

In order to determine damping coefficient, the electromagnetic torque of each measured reading was computed in Table 1 and record the results with rotational velocity in Table 2

Table 2: electromagnetic torque and rotational speed at no load condition

$\omega_m \left(\frac{\text{rad}}{\text{sec}} \right)$	146.6	136	125.6	115.2	94.24	73.30	62.83
$T_m(N.M) = K_t * I_a$	0.0775	0.07595	0.06975	0.062	0.06	0.05735	0.0465

$$B_m = \frac{T_m}{\omega_m} = \frac{\text{average } T_m}{\text{average } \omega_m} = \frac{0.064}{107.68} = 0.00059 \left(\frac{N.M}{\text{rad/sec}} \right)$$

Using an adjustable torque load such as a small practical break coupled to the rotational motor shaft. The torque load was gradually increased to the point where stall occurs. The measuring reading of armature current and speed were taken at different load positions and recorded in table 3. In addition, values of T_L, P_{in}, P_{out} , and efficiency of each measurement data were calculated as shown in the Table 3

Table 3: Experimental measurement data at steady state load condition

Load Position	N (rpm)	$\omega_m \left(\frac{\text{rad}}{\text{sec}} \right) = N(\text{rpm}) * \left(\frac{2\pi}{60} \right)$	$I_a (A)$	Mechanical load torque $T_L(N.M) = K_t I_a - B_m \omega_m$	Input power $P_{in}(w) = V_{in} I_a = 24 I_a$	out power $P_{out}(w) = T_L * \omega_m$	Efficiency $\eta = \left(\frac{P_{out}}{P_{in}} \right) * 100$
0	1300	136.13	0.98	0.0001283	23.52	0.0174	0.07
1	1200	125.66	1.1	0.0778	26.4	9.776	37
2	1150	120.43	1.4	0.0994	33.6	11.97	29.33
3	1050	109.95	1.7	0.1521	40.8	16.72	40.9
4	1000	104.72	2	0.2017	48	21.12	44
5	950	99.48	2.3	0.2513	55.2	24.99	45.27
6	850	89	2.6	0.3040	62.4	27.1	43.42
7	750	78.54	2.9	0.3567	69.6	28.78	41.35
8	700	73.3	3.2	0.4063	76.8	30.78	40
9	650	68.1	3.4	0.4558	81.6	31	37.99
10	600	62.83	3.8	0.4899	91.2	31.5	34.5
11	500	52.36	4.1	0.5581	98.4	29.22	29.69
12	400	41.89	4.4	0.6109	105.6	25.59	24.23
13	350	36.65	4.6	0.6976	110.4	24.2	21.9
14	250	26.18	4.9	0.7471	117.6	18.26	15.52
15	200	20.94	5.6	0.8618	134.4	15.64	11.6
16	100	10.47	5.8	0.873	136.8	9.02	6.59
17	50	5.24	5.9	0.8961	141.6	4.57	3.22
18	0	0	6.1	0.9	146.4	0.009	0

The armature resistance was determined at point where stall torque motor occurs. At this point load torque becomes equal to short circuit torque and the motor can no longer deliver any output. At stall torque, the PMDC motors terminals was fed to 24 volts and the armature current I_a was 6.1A

$$R_a = \frac{V_{in}}{I_a} = \frac{24}{6.1} = 3.93\Omega$$

7. COMPUTER SIMULATIONS

Using derived PMDC motor transfer function, the Simulink model for motor characteristics curves can be obtained. To determine the equations (4) and (11) are transformed into Laplace domain and assume all conditions are zero. See [3] ,[11], [12] and [13].

$$V_a(s) - R_a I_a(s) - S L_a I_a(s) - K_b \omega_m(s) = 0 \dots \dots \dots (20)$$

$$T_L = K_t I_a(s) - J S \omega_m(s) - B_m \omega_m(s)$$

$$K_t I_a(s) - T_L = (J S + B_m) \omega_m(s) \dots \dots \dots (21)$$

From equation (20) $I_a(s)$ can be calculated as

$$I_a(s) = \frac{V_a(s) - K_b \omega_m(s)}{(L_a S + R_a)} \dots \dots \dots (22)$$

Substitute equation (22) in (21)

$$K_t \left(\frac{V_a(s) - K_b \omega_m(s)}{(L_a S + R_a)} \right) - T_L = (J S + B_m) \omega_m(s)$$

$$\frac{K_t V_a(s) - K_t K_b \omega_m(s)}{(L_a S + R_a)} - T_L = (J S + B_m) \omega_m(s)$$

$$\frac{K_t V_a(s)}{(L_a S + R_a)} - \frac{K_t K_b \omega_m(s)}{(L_a S + R_a)} - T_L = (J S + B_m) \omega_m(s) \dots \dots \dots (23)$$

Equation (23) has two inputs $V_a(s)$ and $T_L(s)$ and has one output $\omega_m(s)$. The transfer function from $V_a(s)$ to $\omega_m(s)$ can be derived by setting $T_L = 0$, which gives

$$\frac{\omega_m(s)}{V_a(s)} = \frac{K_t}{(J S + B_m)(L_a S + R_a) + K_t K_b}$$

Similarly, the transfer function from $T_L(s)$ to $\omega_m(s)$ is found by setting $V_a(s) = 0$.

$$\frac{\omega_m(s)}{T_L(s)} = \frac{-(L_a S + R_a)}{(J S + B_m)(L_a S + R_a) + K_t K_b}$$

The output rotational velocity $\omega_m(s)$ is expressed mathematically as

$$\omega_m(s) = \frac{V_a(s) K_t}{(J S + B_m)(L_a S + R_a) + K_t K_b} - \frac{T_L (L_a S + R_a)}{(J S + B_m)(L_a S + R_a) + K_t K_b} \dots \dots \dots (24)$$

The equation (24) can be drawn as a block diagram in Figure 8

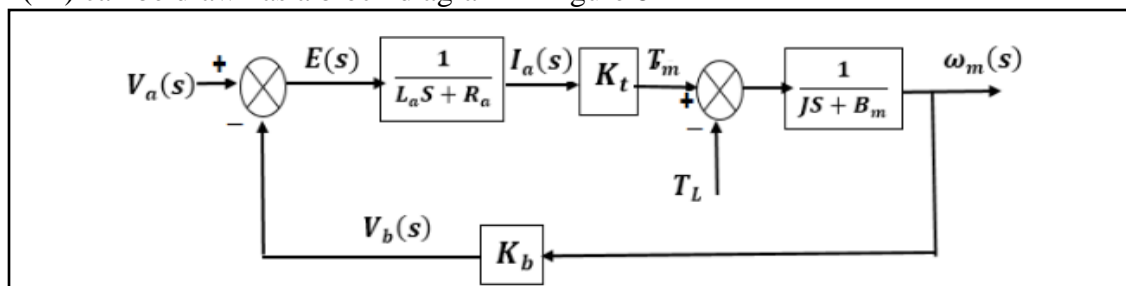


Figure 8: block diagram of equation (24)

The block diagram was implement in Simulink environment in the MATLAB. The model created in Simulink toolbox of MATLAB is shown in Figure 9. The input and output power can be directly computed from Simulink model as shown in Figure 10. To generate the Simulink model at steady state, the functions can be defined in a MATLAB Function block or in the MATLAB command window as

$$R_a = 3.93\Omega, \quad L_a = 0, \quad J = 0, \quad B_m = 0.00059, \quad K_t = K_b = 0.155$$

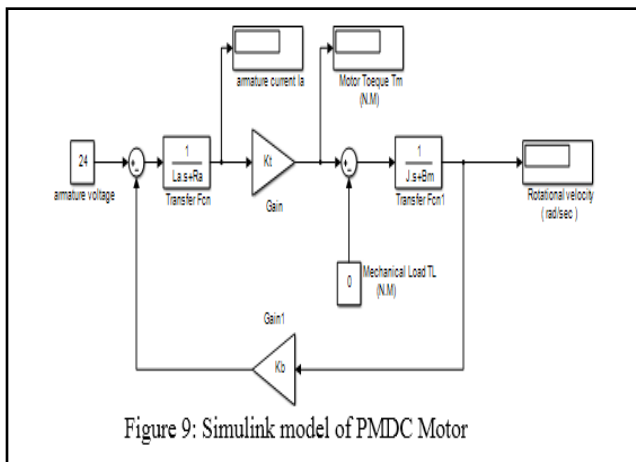


Figure 9: Simulink model of PMDC Motor

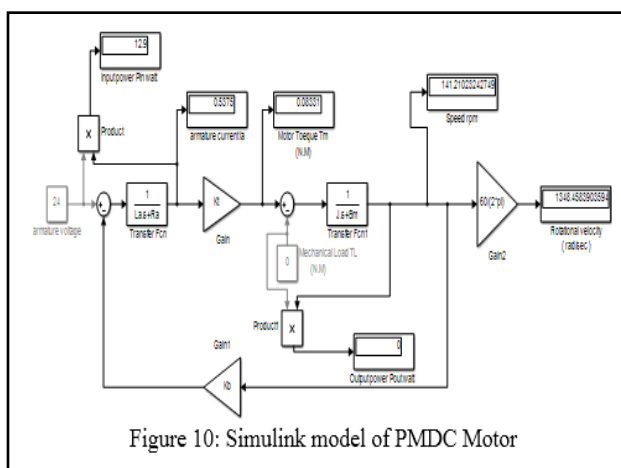


Figure 10: Simulink model of PMDC Motor

After defining functions and gains, Simulink model can be generated at different values for T_L . Measurements data was recorded in Table 4

Table 4: Simulation results

Mechanical load torque $T_L(N.M)$	N (rpm)	$\omega_m \left(\frac{\text{rad}}{\text{sec}}\right) = N(\text{rpm}) * \left(\frac{2\pi}{60}\right)$	$I_a (A)$	Input power $P_{in}(w) = V_{in}I_a = 24I_a$	out power $P_{out}(w) = T_L * \omega_m$	Efficiency $\eta = \left(\frac{P_{out}}{P_{in}}\right) * 100$
0	1300	136.13	0.537	12.9	0	0
0.11	1200	125.66	1.185	28.43	13.73	48.29
0.16	1100	120.43	1.479	35.5	18.77	52.87
0.12	1050	109.95	1.773	42.55	23.08	54.24
0.26	1000	104.72	2.007	49.61	26.63	53.67
0.31	900	99.48	2.36	56.68	29.44	51.94
0.36	850	89	2.66	63.74	31.5	49.41
0.41	800	78.54	2.95	70.8	32.82	46.35
0.46	700	73.3	3.244	77.86	33.39	42.88
0.51	600	68.1	3.54	84.92	33.22	39.11
0.56	550	62.83	3.832	91.98	32.29	35.1
0.61	450	52.36	4.127	99.04	30.63	30.9
0.66	400	41.89	4.421	106.1	28.22	26.59
0.71	350	36.65	4.715	113.2	25.06	22.13
0.76	250	26.18	5	120.2	21.15	17.59
0.81	200	20.94	5.303	127.3	16.5	12.96
0.86	100	10.47	5.598	134.3	11.11	8.27
0.91	50	5.24	5.892	141.4	4.964	3.5
0.9465	0	0	6.106	146.6	0.009	0

To show the difference between experimental test and computer simulations, four characteristics curves are considered important for PMDC motor, which are (1) Torque Vs. armature current, (2) Torque Vs. speed, (3) Torque Vs. output power and (4) Torque Vs. efficiency. These curves were plotted for both experimental and simulation results at load steady state.

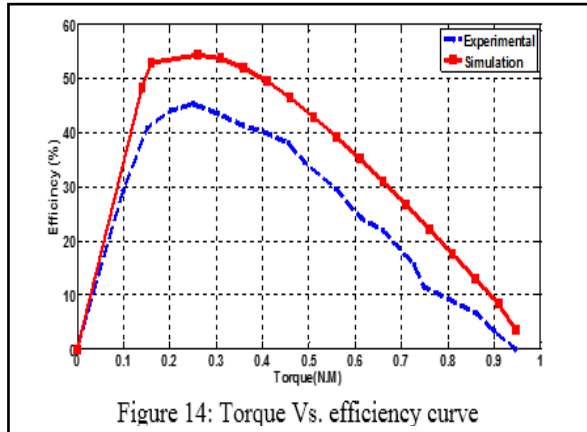
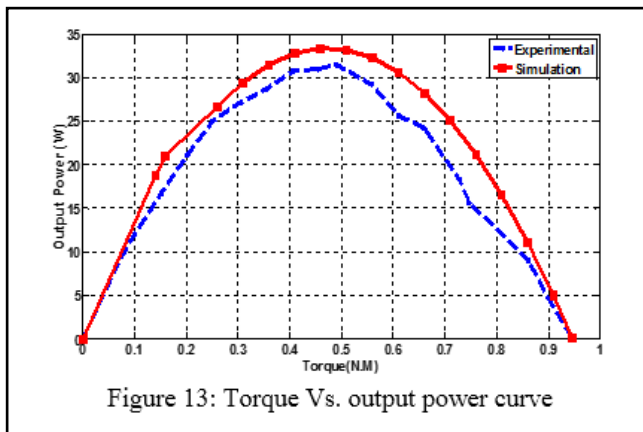
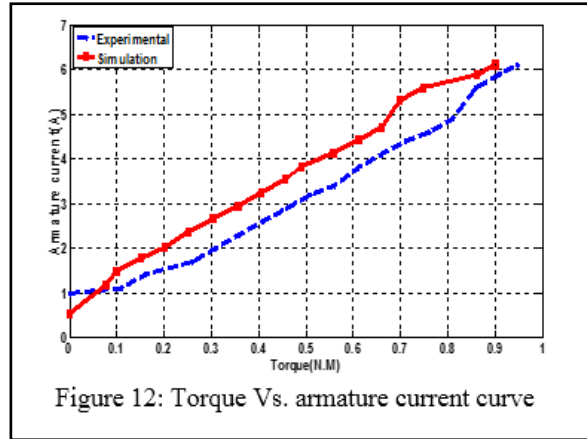
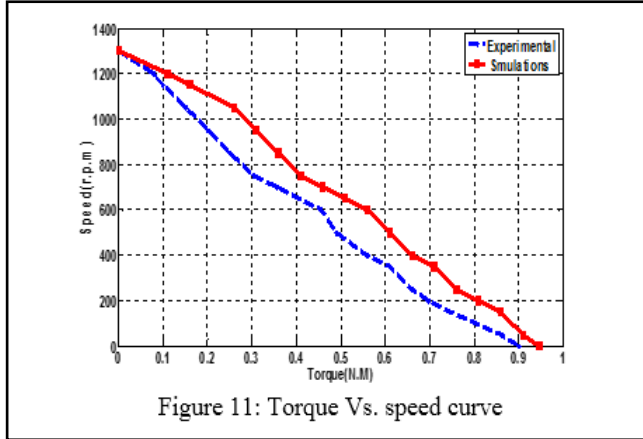


Figure 11 shows the torque is inversely proportional to the speed of the output shaft. At full load, the shaft is not rotating and the torque is at the maximum value, this value is known as a stall torque. At no load the speed of the output shaft is at the maximum value, this means no torque is applied on the output shaft. The curve shown in Figure 12 shows the load torque is directly proportional to the armature current. Figure 13 shows a parabolic curve is a plot of the output power against speed, while Figure 14 shows torque/efficiency curve, it can see that PMDC has high efficiency because there are no field windings and field coil losses. Also, as the stator is provided with a permanent magnet pole system. As you can see from Figures 13 and 14, output power and efficiency curves start from zero at no load condition and end to zero at full load condition, also have maximum value at the point where the armature current is equal to half of its maximum value.

8. CONCLUSION

In this paper, the study was based on the steady state condition. The experimental work was performed on a PMDC and its Simulink model was developed using MATLAB/SIMULINK

Software. The most important conclusions in this paper are PMDC motors have high efficiency and The damping coefficient (B_m) have a negative effect on characteristics of motor especially at no load steady state in spite of smallness value. Furthermore, the results of the study show that there is a close agreement between experimental and simulation results, where experimental results are slightly less than simulation results, this is due to measurement errors in instrumentation and electrical and mechanical losses. Therefore it can use advanced computer software to study the performance of electric machines and understand their behavior and characteristics, especially in the laboratories that lack the presence of equipment.

REFERENCES

- [1] M.G. Say, E.O. Tylor, "Direct Current Machines" Pitman Press, Great Britain, 1982
- [2] S.A. Nasar, "Hand Book of Electric Machines" Mc Graw-Hill, Inc. USA, 1987
- [3] D.O. Anderson, "Modeling DC Electric Motors" Louisiana Tech. University, USA ,
- [4] staff of Festo Didactic "Electricity and New Energy Permanent Magnet DC Motor Courseware Sample" Online. Accessed on 6th July, 2016
- [5] Online electrical engineering study site, "Permanent Magnet DC Motor or PMDC Motor | Working Principle Construction". Online Available: <http://www.electrical4u.com/permanent-magnet-dc-motor-or-pmdc-motor/> Accessed on 5th July, 2016
- [6] Chen JX, Guo YG, Zhou JG, Jin JX, "Performance Analysis of a Surface Mounted Permanent Magnet Brushless DC Motor using an Improved Phase Variable Model", Record of the 2007 IEEE Industry Application Conference, pp. 2169 – 2174.
- [7] Kim CG, Lee JH, Kim HW, Youn MJ, "Study on Maximum Torque Generation for Sensorless Controlled Brushless DC Motor with Trapezoidal Back EMF", IEE Proceedings Electric Power Applications, Vol 152, No 2, March 2005, pp. 277 – 291.
- [8] M. Abdus Salam, "Fundamentals of electrical machines", Narosa Publishing House, USA, 2005.
- [9] H.A. Toliyat, and G.B. Kliman, "Handbook of Electric Motors", CRC Press, USA, 2004.
- [10] W. Lord and J. Hwang, " DC motor model parameters ". IEEE Trans. On Industrial Electronics and Control Instrumentation, vol. IECI-23, No.3, August 1975.
- [11] Ogata K., "Modern Control Engineering" , 2nd ed., Prentice Hall, NJ, 1990.
- [12] Richard C. Dorf, Robert H. Bishop, "Modern Control Systems", Addison Wesley, 2002.
- [13] Norman S. Nise, "Control system engineering", sixth edition, John Wiley & Sons, Inc, 20